



Influence of varying forms of bionic units on repairing remaining quenching surface of gray cast iron

Hui Li^{1,2} · Li Feng^{1,2} · Hong Zhou^{1,2} · Peng Zhang^{1,2} · Ti Zhou³ · Qi Sui^{1,2} · Lu-quan Ren⁴

Received: 6 November 2019 / Revised: 27 February 2020 / Accepted: 2 March 2020 / Published online: 11 June 2020
© China Iron and Steel Research Institute Group 2020

Abstract

In order to repair and reuse remaining quenching surface (RQS) divided into severely worn surface (SWun-S) and mildly worn surface (MWun-S) of abandoned gray cast iron guide rail, inspired by the bionic theory, varying forms of bionic units such as spot (Sp-S), striation (St-S), and reticulation (Re-S) were fabricated on RQS of gray cast iron through laser processing technology. Firstly, the microstructure, phase composition, and microhardness of bionic units and RQS were analyzed by optical microscopy as well as X-ray diffraction instrument and scanning electron microscopy, respectively. Secondly, the oil lubrication wear experiment was performed on homemade line reciprocating wear machine. The results demonstrated that the bionic units had a significant effect on improving wear resistance of RQS of abandoned guide rail due to the microstructure and higher hardness. In addition, the weight loss ratios of MWun-S, Sp-S, St-S, and Re-S samples were decreased by 36.72%, 36.78%, 62.26%, and 80.39%, respectively, compared with that of SWun-S sample. The mechanism of wear resistance enhancement was also discussed.

Keywords Repairing · Laser bionic unit · Remaining quenching surface · Gray cast iron

1 Introduction

Gray cast iron is one of the most commonly used materials for manufacturing machine guide rail, and its reliability plays a vital role in machining accuracy of machine tools due to its easy production, low cost, wear resistance, and anti-vibration performance [1, 2]. According to statistics, almost half of world energy was consumed by a variety of wear [3, 4]. However, under the good oil lubrication condition, friction pairs cannot be completely separated by oil film and also produce wear in the relative motion [5]. As lathe bed and guide rail are regarded as an organic wholeness

for machine tool, once guide rail is abandoned due to wear, meaning that the entire machine tool is also scrapped. Scrapped gray cast iron guide rail brings about a considerable amount of resource consumption and waste every year. The remaining quenching surface (RQS) of abandoned gray cast iron guide rail requires to be repaired and reused, and this not only alleviates environmental contamination but also reduces energy consumption and professional labor used in production. Because guide rail has been utilized frequently, the failure of RQS of gray cast iron was divided into severely worn surface (SWun-S) and mildly worn surface (MWun-S) according to wear degree and hardness with a gradient change along thickness. If the remaining quenching layer is removed to obtain uniform surface, the dimension and precision of guide rail will not meet the requirements of machine tool. Nevertheless, if the remaining quenching layer is retained, it is necessary to explore a simple and new method to repair and reuse RQS of abandoned gray cast iron guide rail.

Laser surface processing is widely used in a great amount of industries, and it holds the advantages of high accuracy and minimum distortion as well as controllability over conventional surface treatment methods. In particular, laser melting technology produces a rapidly

✉ Peng Zhang
pzhjlu@163.com

¹ Key Laboratory of Automobile Materials (Jilin University), Ministry of Education, Changchun 130025, Jilin, China

² School of Material Science and Engineering, Jilin University, Changchun 130025, Jilin, China

³ School of Mechanical and Aerospace Engineering, Jilin University, Changchun 130025, Jilin, China

⁴ Key Laboratory of Terrain Machinery Bionics Engineering (Jilin University), Ministry of Education, Changchun 130025, Jilin, China

solidified layer of high hardness without changing the bulk properties of material, and this also remarkably improves the fatigue strength of materials due to a huge residual compressive stress produced at both sides of the melting region. In the meanwhile, there are a large amount of superior multifunctional structures in the nature that can be used as inspirational systems for the design and synthesis of new and technologically important materials and devices. During the past many years, tremendous efforts have been made to improve the properties of materials by imitating the biological structures of plants, animals, and seashells in nature. For example, the group was dedicated to the investigation of engineering bionic coupling theory [6–10], proving that bionic surfaces could be applied to solve the existing problems such as wear, thermal fatigue, and adhesion failures. The bionic units were manufactured on gray cast iron substrate [11–13] through laser strengthening technique [14] to form the hard phase on the material surface and confirmed that the bionic non-smooth morphology similar to various biological prototypes such as the dung beetle, the ground beetle, the seashell, and the pangolin [15] had a good wear resistance. And this shields lights on a new way to repair and reuse remaining quenching surface of waste gray cast iron guide rail.

In this paper, in order to meet the actual demands of engineering application, varying forms of bionic units were fabricated on RQS of discarded gray cast iron guide rail without consuming additional materials. The microstructure, phase composition, and microhardness of bionic units and RQS were characterized. Then, wear resistance of bionic samples with varying forms was investigated by the man-made reciprocating testing machine in room temperature. By comparison of weight losses, improved wear resistance was found. The mechanism of bionic wear resistance enhancement was also explored.

2 Experimental

2.1 Experimental material

The experimental material was cut from scrapped gray cast iron guide rail. The chemical composition (wt.%) of gray cast iron is listed in Table 1, which is the typical hypoeutectic cast iron. The worn RQS of discarded machine tool guide rail is presented in Fig. 1.

Table 1 Chemical composition of gray cast iron (wt.%)

C	Si	Mn	P	S	Fe
3.25	1.82	0.94	0.15	0.98	Balance

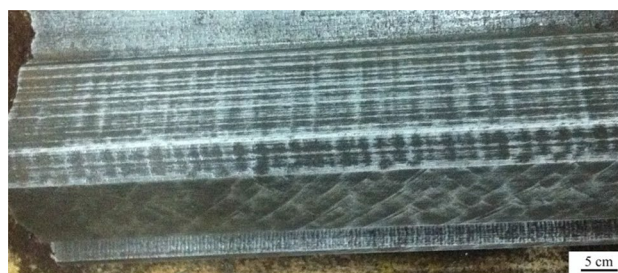


Fig. 1 Worn RQS of discarded machine tool guide rail

2.2 Sample preparation

Samples with the geometrical dimensions of 30 mm × 20 mm × 7 mm were cut from discarded gray cast iron guide rail using the electric spark machine (DK-7732). In order to remove machining marks, the surface and edge of samples were polished by using silicon carbide sandpapers from 60 to 600 grits to obtain ideal surface condition. The samples were ultrasonically rinsed thoroughly with alcohol and acetone before treatment.

A Nd:YAG laser setup with wavelength of 1.064 μm and maximum power of 300 W was adopted to fabricate bionic units with varying forms in this study, and argon gas was used as shielding gas with a constant flow rate of 10 mL/min. First, the processing parameters were fine-tuned. The microstructure of polished weld beads is shown in Fig. 2, and its corresponding laser parameters are indicated in Table 2. Considering the experimental requirements such as no crack and good bonding with substrate, the optimal parameters were as follows: Laser current intensity was 180 A, pulse duration was 6 ms, frequency was 7 Hz, defocusing amount was 12 mm, and scanning speed was 0.42 mm/s. Bionic coupling units are illustrated in Fig. 3, which are spot form, striation form, and reticulation form, and the distance between adjacent units is 4 mm.

2.3 Characterization methods

The microhardness was measured using a Vickers hardness tester (Buehler, 5104, USA) with a load of 2 N and loading time of 10 s at room temperature. X-ray diffraction instrument (XRD, D/Max, 2500PC, Japan) was used to identify phase compositions with Cu Kα radiation ($\lambda = 0.15405$ nm) at a voltage of 40 kV, a current of 40 mA, and a scanning rate of 4 (°)/min. The microstructure of bionic coupling units was characterized by scanning electron microscopy (SEM, Zeiss, EVO18, Germany). Additionally, the worn morphology was observed by optical microscopy (OM,

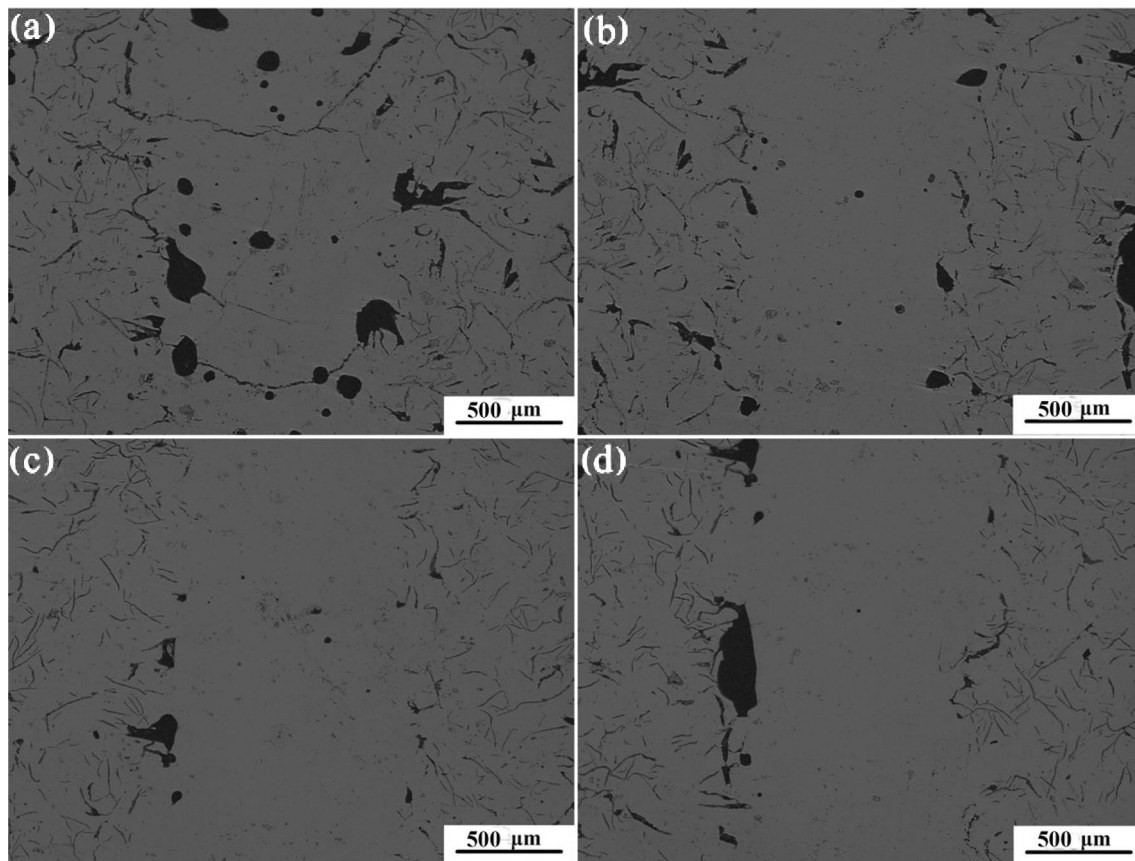


Fig. 2 Typical morphologies of weld beads

Table 2 Laser parameters of weld beads

Sample	Laser current/A	Pulse duration/ms	Frequency/Hz	Defocusing size/mm	Scanning speed/(mm s ⁻¹)
a	180	6	7	11.5	0.5
b	180	6	7	11.5	0.42
c	180	6	7	12	0.42
d	180	6	7	14	0.42

OLYMPUS, PMG3, Japan) and three-dimensional surface scanning profiler (Wyko NT9100, Japan).

2.4 Wear experiment

There were five kinds of samples named spot (Sp-S), striation (St-S), reticulation (Re-S), severely worn untreated surface (SWun-S), and mildly worn untreated surface (MWun-S) samples. Before oil wear experiments, all the samples were immersed in oil for 3 days so that samples fully absorbed a lot of lubricating oil. In order to investigate sliding wear performance, the homemade linear

reciprocating wear machine was applied to experiments, and its schematic is illustrated in Fig. 4. The eccentric wheel was put in motion along with the rotation of gear reducer driven by electromotor, which made the friction pairs go on straight line reciprocating movement along with the connecting rod. The speed of wear test was controlled by frequency converter, which was linked with electromotor. The pressure of wear test was controlled through changing the load. The speed of wear test was 690 r/min, and the applied load was 80 N. The samples were cleaned by alcohol in an ultrasonic cleaner after wear experiment of 60 h. The electronic balance (FA2004) with a precision of 0.0001 g was used to measure the weight of samples before and after wear test. The weight of samples was measured three times and then taken the average value with six decimal places. Additionally, it required to eliminate residual oil inside to ensure the accuracy of weight loss. Therefore, sample height was named as h_1 and sample weight was named as m_1 before immersed in oil, sample weight was named as m_2 after immersed in oil, and sample height was named as h_2 and sample weight was named as m_3 after wear experiment of 60 h. The pure weight loss Δm was calculated by the following equation:

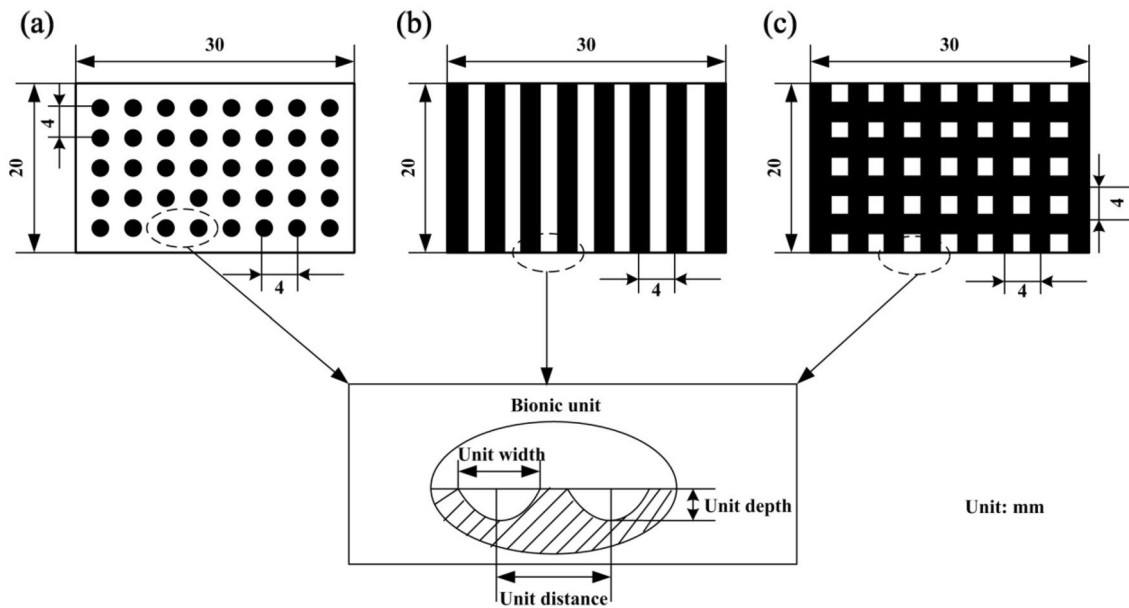


Fig. 3 Sketch of bionic samples. **a** Spot unit; **b** striation unit; **c** reticulation unit

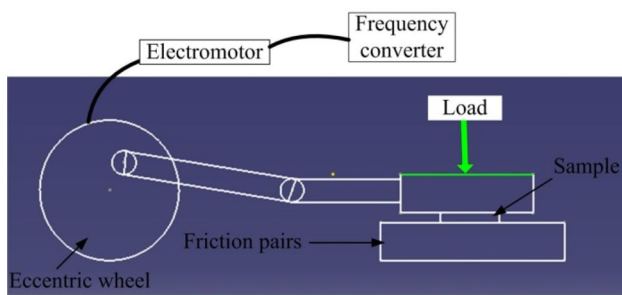


Fig. 4 Schematic of homemade linear reciprocating wear machine

$$\Delta m = m_1 - m_3 - (m_2 - m_1)h_2/h_1 \quad (1)$$

3 Results and discussion

3.1 Hardness of RQS of gray cast iron

The schematic of cross-section hardness measurement of RQS in worn sample is shown in Fig. 5. And the hardness curve along with thickness is indicated in Fig. 6. It can be seen from the curve that the hardness declined with an increase in quenching layer thickness. When the thickness was less than 1.5 mm, hardness was approximate to 800 HV. When the thickness is between 1.5 and 3.0 mm, there was an approximately linear relationship between the hardness and thickness. However, when the thickness was larger than 3.0 mm, the hardness was about 250 HV. In general, the

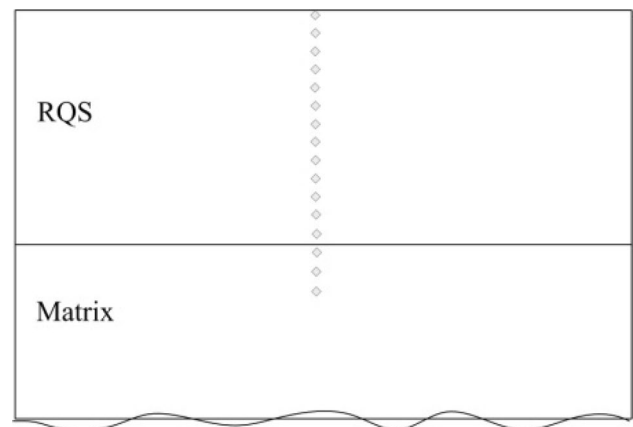


Fig. 5 Schematic of cross-section hardness measurement of worn sample

hardness of RQS was 450–600 HV which was much higher than that of gray cast iron matrix. As the structure could determine hardness and the hardness in turn could explain the structure, it could be inferred that the structures of RQS and gray cast iron matrix were different and it was necessary to analyze the microstructure of RQS of gray cast iron.

3.2 Morphology and microstructure of RQS and bionic unit

XRD analysis of RQS and laser bionic unit is presented in Fig. 7, in which Fig. 7a shows XRD pattern of RQS and Fig. 7b shows that of bionic unit. The original microstructure of RQS was martensite + residual austenite + graphite. The

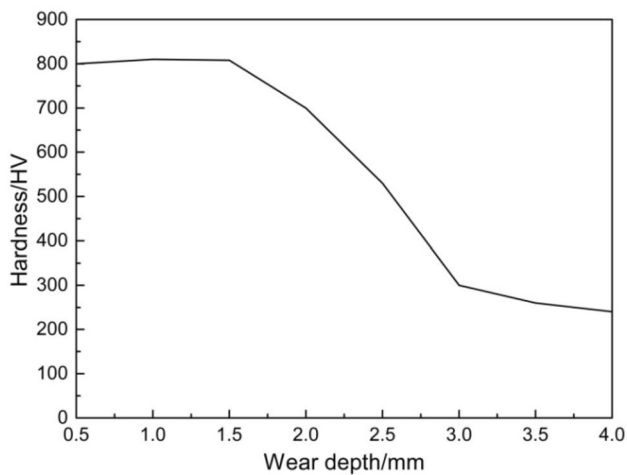


Fig. 6 Hardness curve of RQS of gray cast iron at different depths

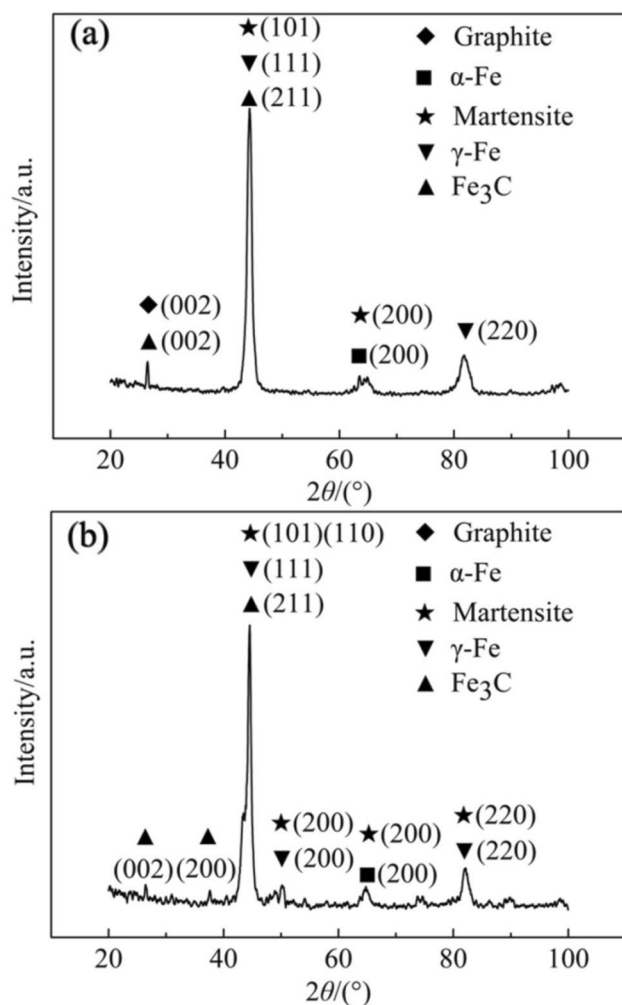


Fig. 7 XRD analysis of RQS (a) and bionic unit (b)

transformation was incomplete for restriction of the carbon solution. However, it can be seen that there was no graphite in the bionic unit zone. Austenite, formed at high temperature, was correspondingly transformed into martensite due to a high solidification rate. And a large amount of martensite formation was confirmed by XRD pattern, as shown in Fig. 7b.

The corrosion result of RQS of worn sample was observed by OM, as shown in Fig. 8a. From the analysis of Figs. 7a and 8a, the microstructure of RQS consisted of martensite (M), residual austenite (RA), a part of pearlite (P), and flake graphite (G). Here, austenite, pearlite, ferrite, and other microstructures around graphite or eutectic carbides were all called substrate. RQS of worn sample without corrosion is indicated in Fig. 8b. The supercooling eutectic graphite (D type), chrysanthemum-shaped graphite (B type), and irregular graphite (A type) were found. In order to obtain good mechanical properties, A-type graphite or a small amount of graphite similar to B-type graphite was ideal. Nevertheless, it was the best without D-type graphite. As severely worn surface had D-type graphite, it explained why performance of severely worn sample was bad.

It can be seen from Figs. 7b and 9 that the microstructure of laser bionic unit was martensite + remaining austenite. During the process of obtaining the bionic unit, light energy and heat energy were exchanged between laser and gray cast iron. As the light energy was absorbed, the surface of gray cast iron was rapidly melted through the thermal conduction and subsequently solidified under a fast cooling rate resulting from the cold surrounding unfused areas to provide the bionic unit. The nucleation rate was higher than the growth rate due to fast heating and high supercooling. Furthermore, martensitic diffraction peak of laser bionic unit was wider than that of RQS, which indicated that crystal grains in the whole unit zone were very fine and compact, as shown in Fig. 9.

3.3 Relationship between microstructure and hardness

In order to make hardness as accurate as possible and eliminate interference of accidental factors, multi-angle and multi-point measurement should be conducted; namely, twenty points were selected in every sample and every point was measured clockwise for three times. Then, we removed the inaccurate measurements and took the average value of the rest. Figure 10a–d shows hardness of RQS of SWun-S, Sp-S, St-S, and Re-S samples, while Fig. 10e–h shows the hardness of bionic units of Sp-S, St-S, Re-S, and Re-S, where Fig. 10g is from the non-joint and Fig. 10h is from the joint (as shown in Fig. 11). The hardness of Re-S non-joint was 777.3 HV and that of Re-S joint was 816.2 HV. The hardness of Re-S was

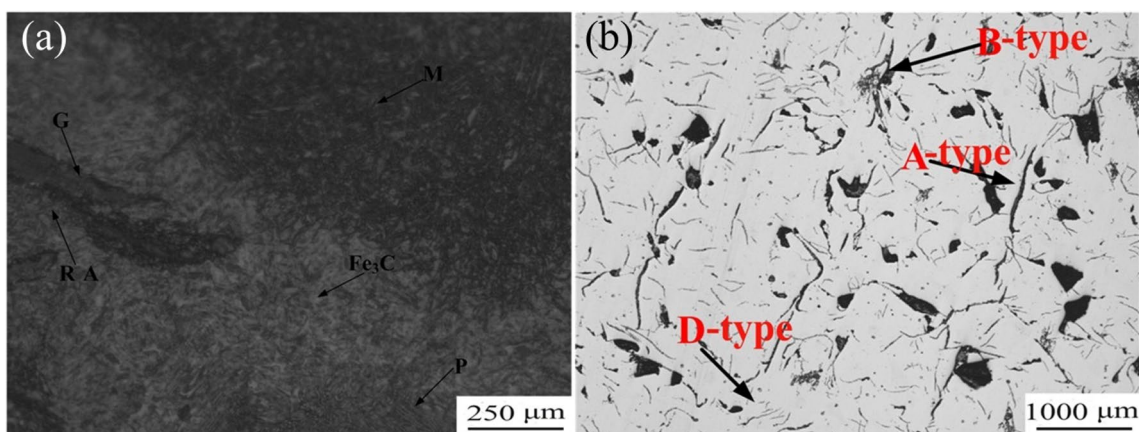


Fig. 8 Morphology of RQS of sample with corrosion (a) and without corrosion (b)

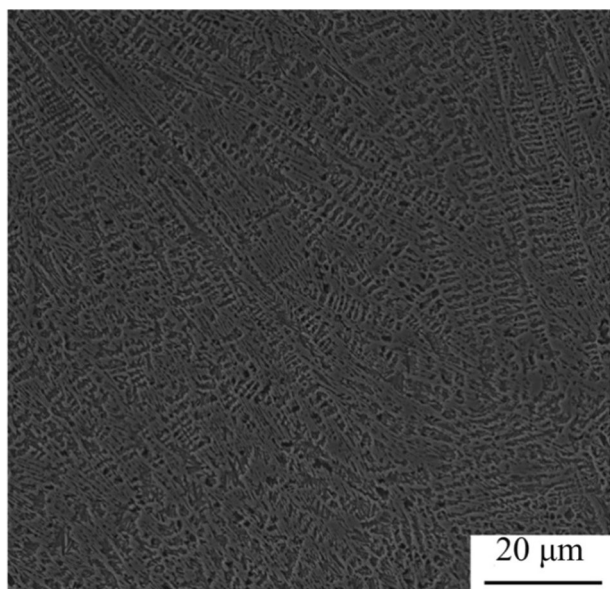


Fig. 9 Microstructure of bionic coupling unit

the average value of the non-joint and the joint, namely 788.9 HV. Hardness values of Sp-S, St-S, Re-S, and RQS are also illustrated in Fig. 12. The average values of hardness of the bionic units (Sp-S, St-S, Re-S) were increased by 12.8%, 24.8%, and 28.5% compared to the hardness of RQS, respectively. Therefore, laser bionic units had a higher hardness. From Sect. 3.2, bionic units by laser processing could obtain more uniform and finer martensite. Martensitic transformation, grain refinement, and dispersion strengthening could make hardness increase [16], so that the fine martensite grain and the residual compressive stress produced by laser processing made the hardness of bionic units higher. As for the reason why the hardness of Re-S joint was higher than that of the non-joint, it might

be attributed to material fused twice by laser which made material phase transformation more thorough and grain further refined.

3.4 Oil wear results

According to the definition of Δm mentioned above in Sect. 2.4, the net weight loss of SWun-S, MWun-S, Sp-S, St-S, and Re-S samples was calculated after wear of 60 h, and all datum and results are listed in Table 3. Then, combined with previously accumulated data of the group [17], wear results with six decimal places as units of the substrate and RQS of gray cast iron are gathered in Table 4, where the weight loss of sample with spot bionic unit was defined as Δm_{Sp} , the weight loss of sample with striation bionic unit was defined as Δm_{St} , and the weight loss of sample with reticulation bionic unit was defined as Δm_{Re} . It could be found that weight losses of gray cast iron RQS with bionic units were relatively smaller. This illustrates that bionic units of RQS showed better wear resistance, which further explains the feasibility of the experiment. Therefore, it was better to keep remaining quenching layer.

The weight loss histogram of SWun-S, MWun-S, Sp-S, St-S, and Re-S samples is shown in Fig. 13. It can be seen that weight loss of SWun-S sample was the largest, weight loss of bionic sample was much smaller, and the weight loss of Sp-S sample was approximate to that of MWun-S sample. Then, the reduction percentage (X) of weight loss was applied to estimate wear resistance of bionic coupling samples, which was defined as follows:

$$X = (\Delta m_{SWun} - \Delta m_x) / \Delta m_{SWun} \times 100\%, \quad (2)$$

where Δm_{SWun} is the weight loss of SWun-S sample; and Δm_x stands for the weight loss of MWun-S, Sp-S, St-S, and Re-S samples, respectively. The reduction percentages of

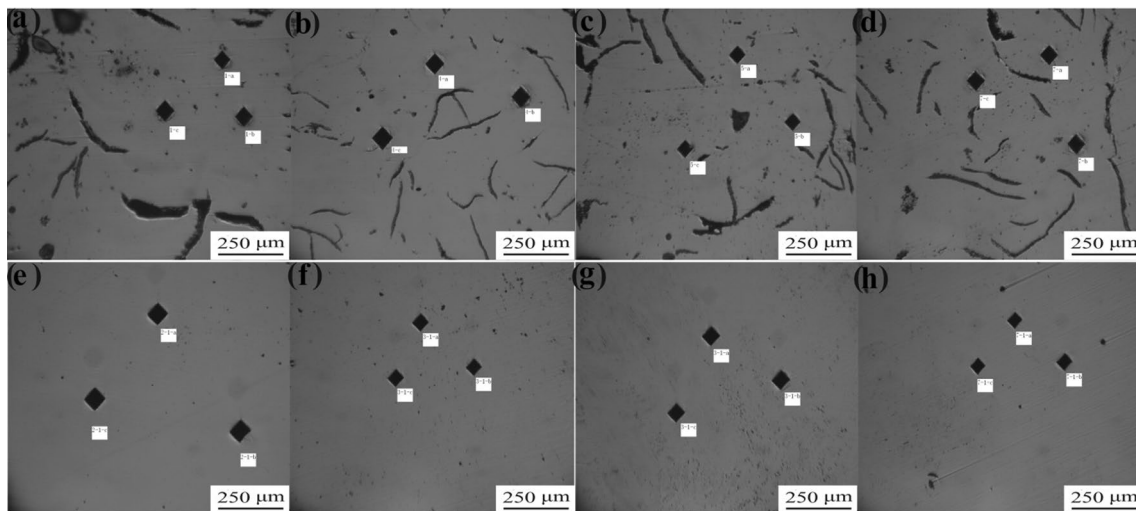


Fig. 10 Schematic diagram of hardness measurement

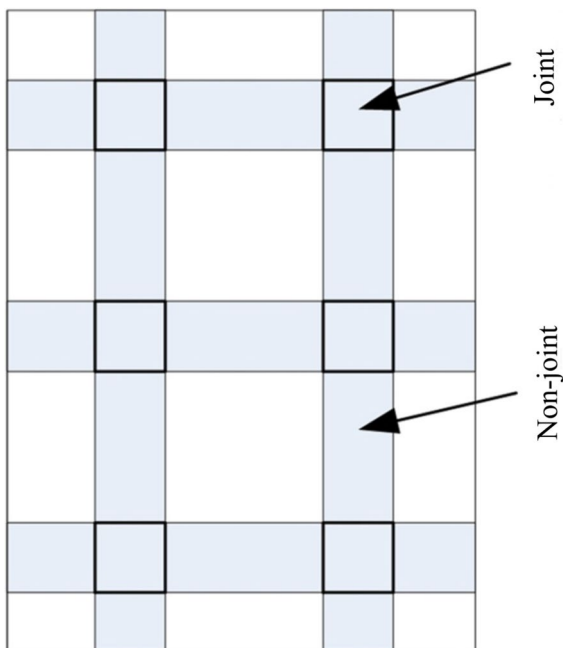


Fig. 11 Schematic of joint and non-joint of reticulation unit

weight loss of MWun-S, Sp-S, St-S, and Re-S samples were 36.72%, 36.78%, 62.26%, and 80.39%, respectively, compared with that of SWun-S sample. As the reduction percentages of weight loss of bionic samples were larger than that of MWun-S sample, RQS of gray cast iron with bionic units exhibited better wear resistance. Since mildly worn surface of guide rail could work normally, it might infer that severely worn surface with laser bionic units could also work normally under the same wear condition. This result demonstrates that the existence of bionic coupling units was beneficial to improving the wear resistance of gray cast iron

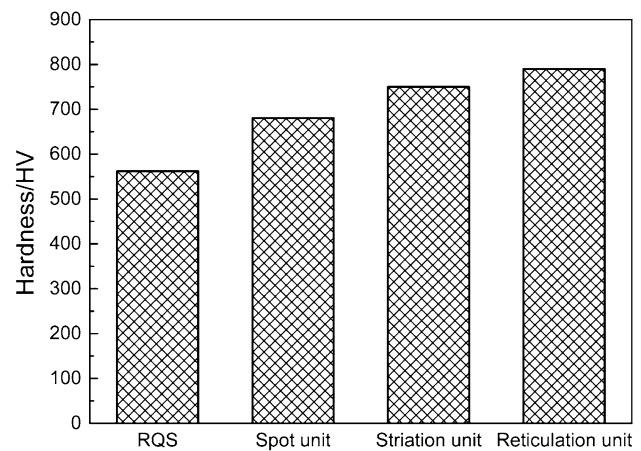


Fig. 12 Hardness of bionic units and RQS

RQS, and it could also meet the requirements of repairing and reusing discarded machine tool guide rail.

3.5 Bionic wear resistance mechanism

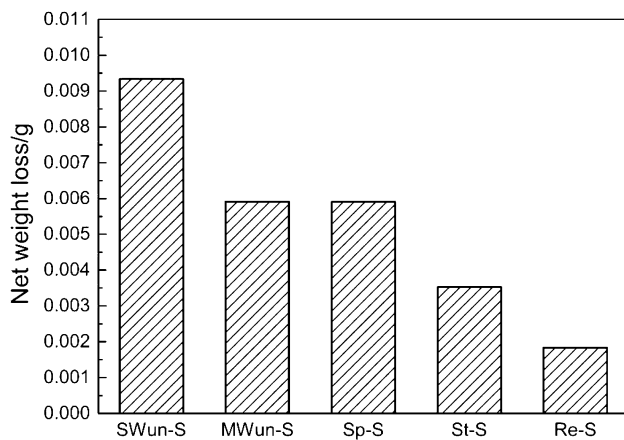
From the above results of wear experiment, bionic units had the advantages of repairing and reusing discarded machine tool guide rail. Coupled with the worn morphology of the sample as shown in Fig. 14a, b, it could analyze the reason why bionic units could improve the resistance to wear. First, laser bionic units had a higher hardness. Secondly, bionic units could be regarded as the hard phase to provide strength due to martensite transformation and grain refinement, while the rest could be regarded as the soft phase to provide ductility, toughness, and shock absorption. The alternating action of the hard phase and the soft phase could ensure stability of gray cast iron guide rail.

Table 3 Datum and results of different samples

Sample	h_1/mm	m_1/g	m_2/g	h_2/mm	m_3/g	$\Delta m/\text{g}$
SWun-S	6.72	26.78703	26.790166	6.70	26.780817	0.00933968
MWun-S	6.88	26.46807	26.472267	6.84	26.466333	0.00590958
Sp-S	7.12	27.52350	27.529100	7.10	27.523180	0.00590427
St-S	7.16	27.62033	27.633233	7.10	27.629600	0.00352490
Re-S	7.42	28.15547	28.168600	7.40	28.166733	0.00183160

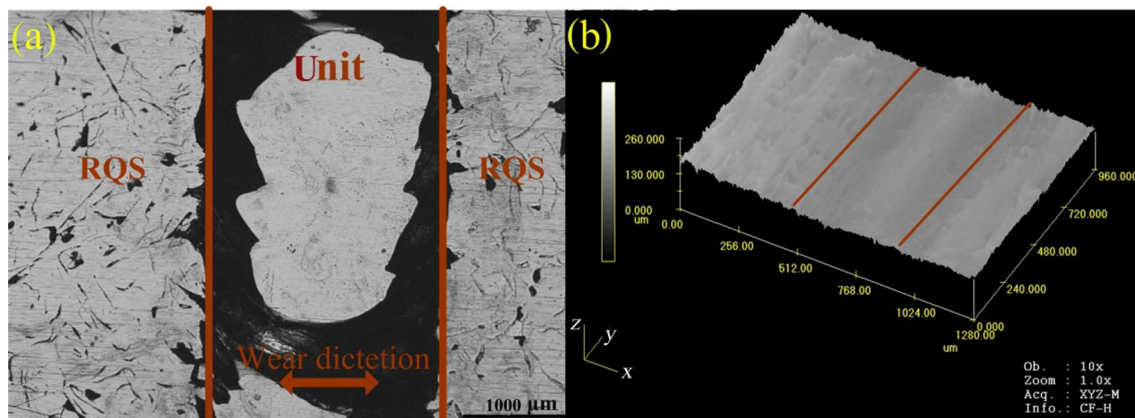
Table 4 Wear results with bionic units on gray cast iron substrate and RQS

Sample	$\Delta m_{Sp}/\text{g}$	$\Delta m_{St}/\text{g}$	$\Delta m_{Re}/\text{g}$
Substrate	0.006254	0.005125	0.004100
RQS	0.005904	0.003525	0.001832

**Fig. 13** Histogram of weight loss of remaining quenching surface

The main wear mechanism was adhesive wear. The worn degree of the soft phase was greater than that of the hard phase along with wear experiments, and then, the hard phase provided main support to reduce wear of the soft phase, leading to the improvement of wear resistance. In the beginning of the wear process, bionic units and substrate were in the same plane (Fig. 15a). When the bionic units moved on the wear pair surface, the wear pair surface near the contacting part produced a certain plastic deformation due to the large pressure between them, which broke the substrate surface near the bionic units. Compared with the hard phase unit, the wear debris was ground off by the unit when it moved to the hard phase bionic unit. The units could bear the abrasion only until the height difference reached equilibrium position (Fig. 15b).

Bionic units also had the advantages of reducing crack initiation and hindering crack propagation [18]. A seriously worn surface had the drawback of pitting which resulted in crack initiation. However, there was a less possibility of crack initiation due to bionic units without pitting. Once the crack of remaining quenching region extended to bionic units, crack propagation would be hindered or stopped due to bionic units with higher hardness. It demonstrated that bionic units could retard the removal of material and the abrasive action produced

**Fig. 14** OM worn morphology (a) and 3D worn morphology by surface profiler (b)

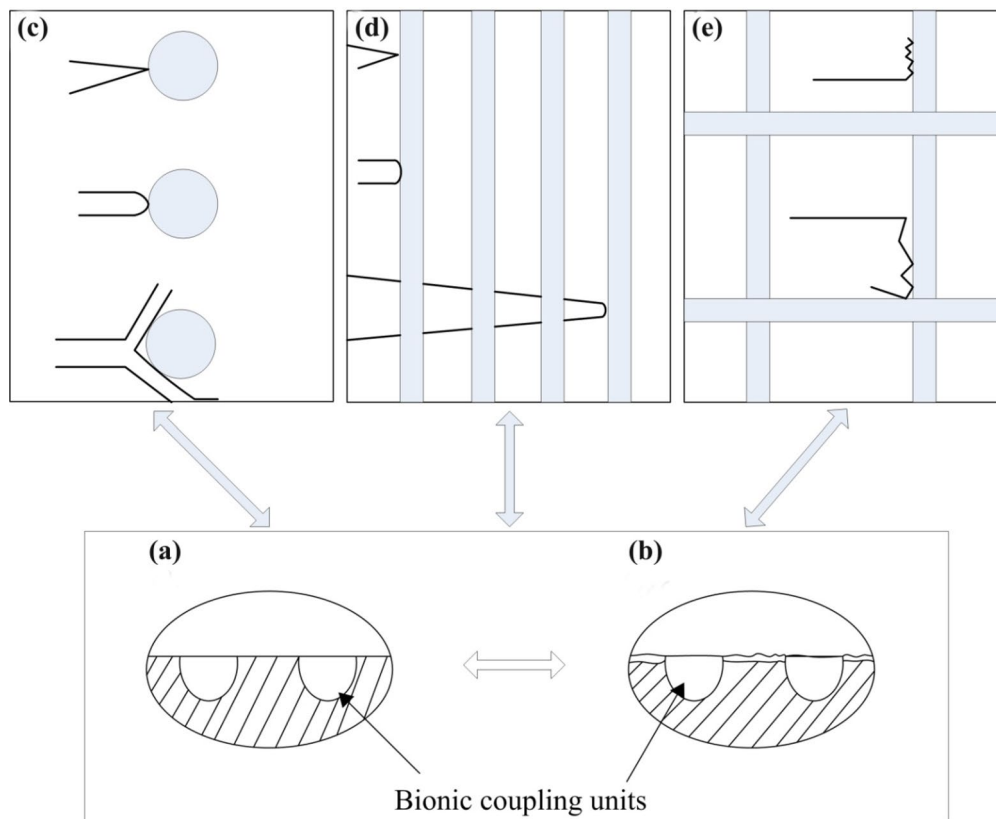


Fig. 15 Modes for wear mechanism and crack retardation mechanism of bionic sample. **a** Initial wear process; **b** later wear process; **c** spot bionic unit; **d** striation bionic unit; **e** reticulation bionic unit

by the debris could be prohibited in the meantime. The crack retardation mechanism of bionic units with pile–nail effect is shown in Fig. 15c–e. It indicated that the bionic units could have a superior deformation resistance. On the one hand, the striation units similar to the bridges gave more additional support. On the other hand, the reticulation units similar to a combination of bridges and dams were effective to improve the wear behavior of the sample. Owing to the existence of varying forms of bionic units, it will decrease the accumulation of plastic deformation to reduce the stress concentration and more energy is needed for crack propagation in the unit zone. Hence, it not only can cause such advantaged inhibition to crack propagation, but also can postpone the crack initiation that is attributed to the refinement microstructure. Moreover, the samples exhibited significantly improved wear resistance, and this also could meet the requirements of repairing and reusing gray cast iron RQS of abandoned machine tool guide rail.

4 Conclusions

1. Laser processing method provided significant increase in the microhardness of the bionic units. The average hardness values of bionic units with varying forms (spot, striation, and reticulation) were increased by 12.8%, 24.8%, and 28.5%, respectively, compared with that of the gray cast iron RQS. The superior mechanical property of the bionic units was attributed to the combined strengthening effects of martensite transformation and grain refinement.
2. The varying forms of bionic units by laser technique led to a significant improvement in the wear resistance compared with RQS of gray cast iron, characterized by lower wear loss. The weight loss ratios of MWun-S, Sp-S, St-S, and Re-S samples were decreased

by 36.72%, 36.78%, 62.26%, and 80.39%, respectively, compared with the net weight loss of SWun-S sample.

3. Bionic coupling units could also hinder crack initiation and crack propagation. Furthermore, it was simple and convenient without consuming additional material, which could reach the purpose of repairing and reusing gray cast iron RQS of abandoned machine tool guide rail.

Acknowledgements This work was supported by Project 985-High Performance Materials of Jilin University, Project 985-Bionic Engineering Science and Technology Innovation and double first-class project by Jilin Province and Jilin University (SXGJXX2017-14).

References

- [1] Z.K. Chen, T. Zhou, H.F. Zhang, W.S. Yang, H. Zhou, J. Mater. Eng. Perform. 24 (2015) 2511–2520.
- [2] Z.B. Pang, H. Zhou, P. Zhang, D.L. Cong, C. Meng, C.W. Wang, L.Q. Ren, Appl. Surf. Sci. 331 (2015) 179–184.
- [3] H.P. Jost, Wear 136 (1990) 1–17.
- [4] J. Gou, Z.J. Liu, H. Jia, J. Iron Steel Res. Int. 25 (2018) 243–251.
- [5] Q. Sui, H. Zhou, L. Yang, G.Y. Liang, H.F. Zhang, P. Zhang, Z.K. Chen, Tribol. Int. 117 (2018) 180–188.
- [6] L. Chen, L.Q. Ren, Y. Zhao, H. Zhou, J. Bionic Eng. 5 (2008) 34–39.
- [7] Z.B. Pang, H. Zhou, G.F. Xie, D.L. Cong, C. Meng, L.Q. Ren, Opt. Laser Technol. 70 (2015) 89–93.
- [8] Z.H. Zhang, H. Zhou, L.Q. Ren, X. Tong, H.Y. Shan, Y. Cao, Appl. Surf. Sci. 253 (2007) 8939–8944.
- [9] H. Zhou, X. Tong, Z.H. Zhang, X.Z. Li, L.Q. Ren, Mater. Sci. Eng. A 428 (2006) 141–147.
- [10] H.Y. Shan, H. Zhou, N. Sun, L.Q. Ren, L. Chen, X.Z. Li, J. Mater. Process. Technol. 199 (2008) 221–229.
- [11] A. Blarasin, S. Corcoruto, A. Belmondo, D. Bacc, Wear 86 (1983) 315–325.
- [12] X. Tong, H. Zhou, L.Q. Ren, Z.H. Zhang, R.D. Cui, W. Zhang, Surf. Coat. Technol. 202 (2008) 2527–2537.
- [13] Z.K. Chen, T. Zhou, R.Y. Zhao, H.F. Zhang, W.S. Yang, H. Zhou, P. Zhang, L.Q. Ren, J. Mater. Res. 30 (2015) 3104–3115.
- [14] J. Lawrence, L. Li, Surf. Coat. Technol. 140 (2001) 238–240.
- [15] Z.W. Han, Z.Z. Mu, W. Yin, W. Li, S.C. Niu, J.Q. Zhang, L.Q. Ren, Adv. Colloid Interf. Sci. 234 (2016) 27–50.
- [16] Y. Gao, Influence of forms and characteristics of bionic coupling units on cast iron under oil sliding, Jilin University, Changchun, China, 2015.
- [17] A. Hidouci, J.M. Pelletier, F. Ducoin, D. Dezert, R. El Guerjouma, Surf. Coat. Technol. 123 (2000) 17–23.
- [18] S. Kamat, X. Su, R. Ballarini, A.H. Heuer, Nature 405 (2000) 1036–1048.